

**Cell Host & Microbe, Volume 28**

**Supplemental Information**

**Cholesterol Metabolism**

**by Uncultured Human Gut Bacteria**

**Influences Host Cholesterol Level**

**Douglas J. Kenny, Damian R. Plichta, Dmitry Shungin, Nitzan Koppel, A. Brantley Hall, Beverly Fu, Ramachandran S. Vasan, Stanley Y. Shaw, Hera Vlamakis, Emily P. Balskus, and Ramnik J. Xavier**

## SUPPLEMENTAL INFORMATION

### SUPPLEMENTAL FIGURES

**Figure S1.** Replication of bioinformatic analysis of assembled human gut microbiome gene catalogue in an independent dataset with paired stool metagenomes and metabolomes along with further analysis of the clusters of proteins with homology to proteins encoded by gut microbes previously implicated in coprostanol formation.

**Figure S2.** Cholesterol metabolism by *Eubacterium coprostanoligenes* in pure culture and lysates; in vitro activity of purified N-terminal His-tagged ECOP170 expressed in *E. coli* BL21(DE3); and mechanism and catalytic residues for hydroxysteroid dehydrogenases.

**Figure S3.** Identification of human-associated cholesterol dehydrogenases with homology to IsmA in the combined assembly of gut metagenomes from six human cohorts.

**Figure S4.** IsmAs from human-associated gut microbes metabolize cholesterol and coprostanol but not primary bile acids.

**Figure S5.** IsmA-encoding species identified across 6 human gut microbiome cohorts are related to known *Clostridium* species and are associated with coprostanol formation in ex vivo stool cultures.

**Figure S6.** Quantitative targeted metabolomics of cholesterol, cholestenone and coprostanol in a subset of stool samples from the PRISM cohort.

## SUPPLEMENTAL FIGURES

**Figure S1. Replication of bioinformatic analysis of assembled human gut microbiome gene catalogue in an independent dataset with paired stool metagenomes and metabolomes along with further analysis of the clusters of proteins with homology to proteins encoded by gut microbes previously implicated in coprostanol formation, related to Figure 2. (A-D)** Legend as in Fig. 2, apart from value in panel (A) where 2.5% of protein clusters are found with greater than 50% specificity and sensitivity. **(E)** Clusters containing proteins with >50% AA identity to a protein found within a specified organism were highlighted on the association figure generated for two independent human cohorts, dataset 1 (PRISM) and dataset 2 (HMP2). **(F)** Scores of sensitivity in relation to presence of coprostanol were very low when calculated for each member of the cluster of homologous proteins that was confirmed to contain cholesterol dehydrogenase enzymes (compare with sensitivity for cluster marked as ECOP170 in Fig. 2D and Fig. S1D).

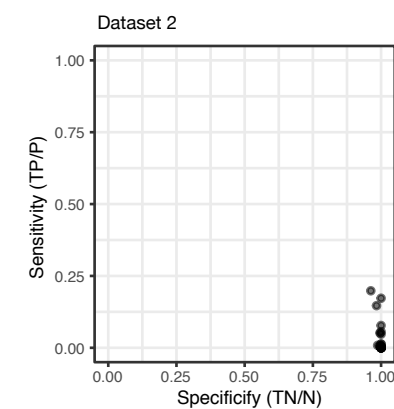
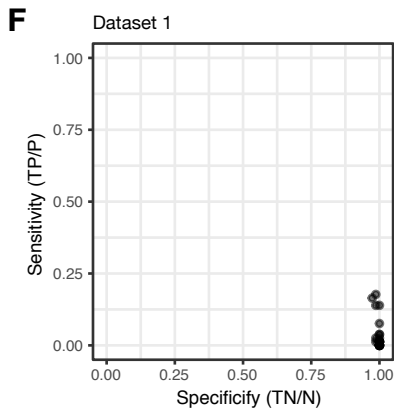
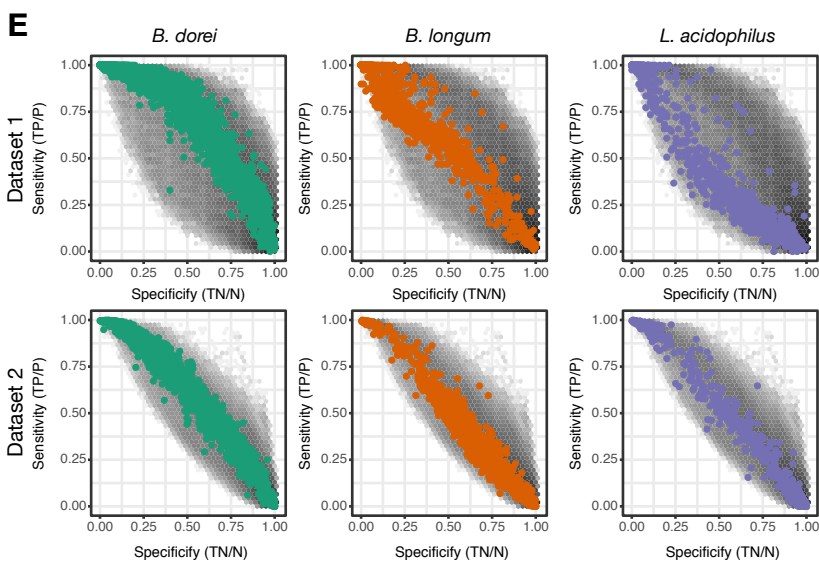
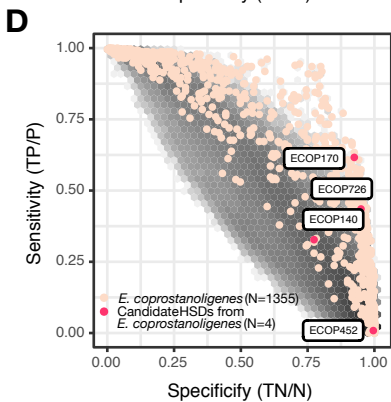
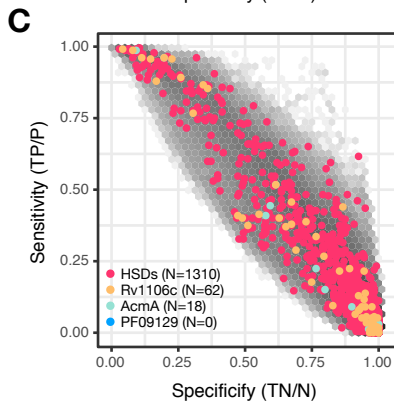
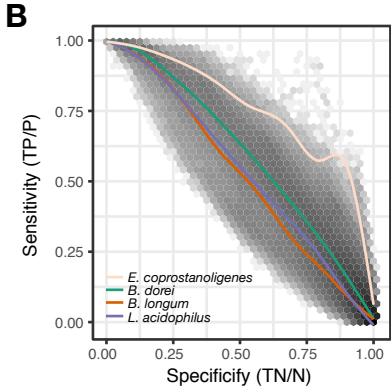
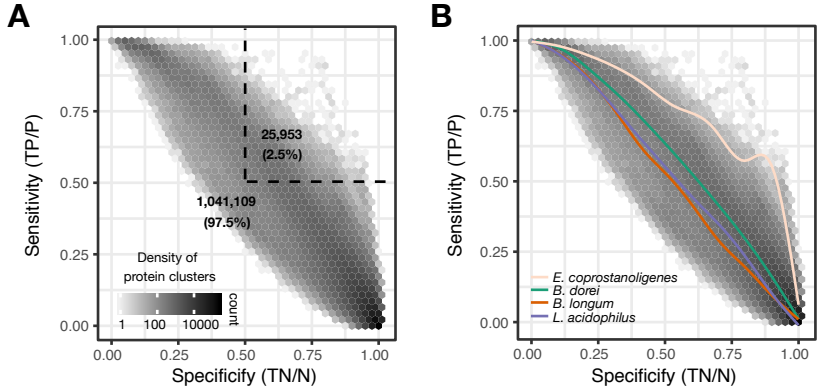
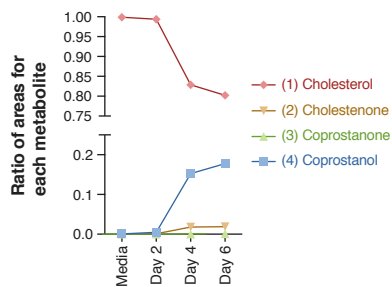


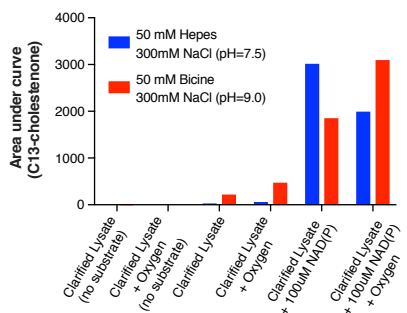


**Figure S2. Cholesterol metabolism by *Eubacterium coprostanoligenes* in pure culture and lysates and *in vitro* activity of purified N-terminal His-tagged ECOP170 expressed in *E. coli* BL21(DE3), related to Figure 3. (A)** *E. coprostanoligenes* was cultured for 6 days in basal cholesterol medium under anaerobic conditions at 37 °C. At days 2, 4 and 6, samples were taken from the culture and levels of cholesterol and downstream metabolites were quantified using LC-MS. **(B)** Activity assay in *E. coprostanoligenes* clarified lysate after growth for 2 days in media with 2 different buffer conditions. Conversion of cholesterol (100 μM) to cholestenone when a mixture of NAD<sup>+</sup> and NADP<sup>+</sup> (100 μM) is added to the clarified lysate occurs in both anaerobic and aerobic assay conditions after overnight incubation in both buffer conditions. **(C)** Activity assay in *E. coprostanoligenes* lysate after growth for 2 days in media without cholesterol and lysis under anaerobic conditions. Conversion of cholesterol (100 μM) to cholestenone occurs under anaerobic conditions in HEPES (50mM, pH = 7.5, 300 mM NaCl) when NADP<sup>+</sup> (100 μM) is added to the lysate. Extracted ion chromatograms (EICs) of **2** (rt 2.60, 385.244 → 108.988) are shown for all conditions. **(D)** The expression levels of the four genes encoding putative HSDs in *E. coprostanoligenes* when grown in cholesterol containing medium compared to medium without cholesterol at 48 h by qPCR. *ECOP170* is the HSD with the highest fold change in expression when *E. coprostanoligenes* is grown on cholesterol containing medium compared to medium without cholesterol. Each point represents a biological replicate with the center bar representing the mean and error bars represent s.d. (*n* = 3). *P* values were determined by one-way ANOVA followed by Tukey's multiple comparisons test. **(E)** N-terminal His<sub>6</sub>-tagged protein was purified with Ni-NTA Agarose (Qiagen) **(F)** Activity assay with varying concentrations of ECOP170 in HEPES (pH = 7.5, 50 mM, 300 mM NaCl) with 100 μM cholesterol and either 200 μM of NADP<sup>+</sup> (left) or 200 μM of NAD<sup>+</sup> (right) after 10, 20 and 30 min. EICs of **2** (rt 2.60, 385.244 → 108.988) are shown for all conditions. **(G)** Putative mechanism for the oxidation of cholesterol to cholestenone by cholesterol dehydrogenase. **(H)** SDS-PAGE gel showing expression of ECOP170 containing point mutants in *E. coli* BL21. **(I)** Mutagenesis of ECOP170 shows the predicted active site residues S138, Y151 and K155 are required for conversion of cholesterol to cholestenone.

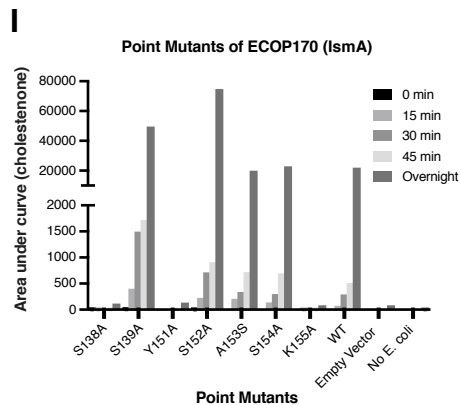
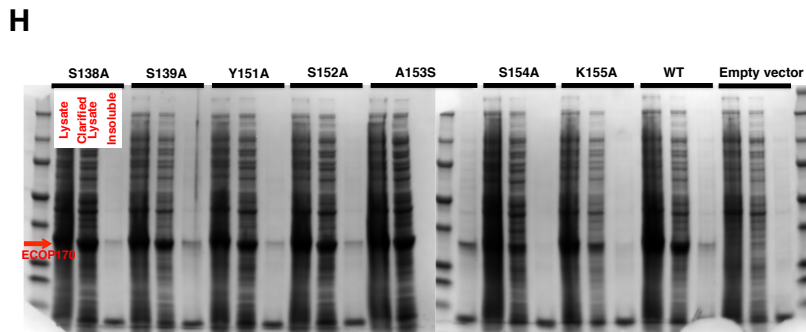
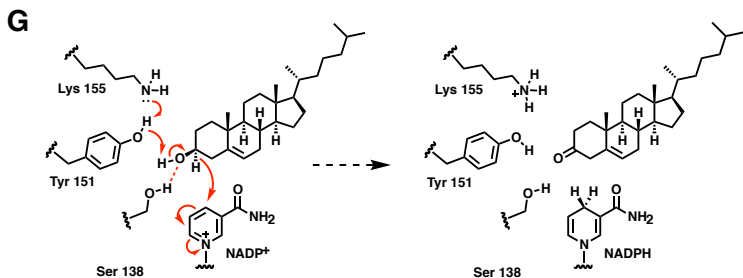
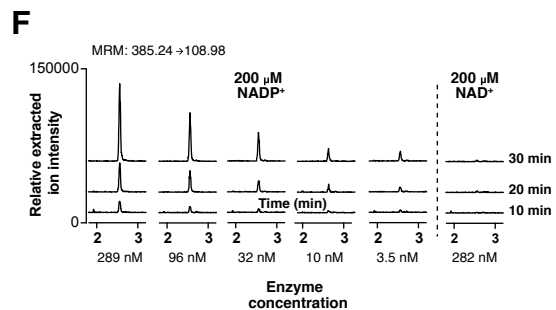
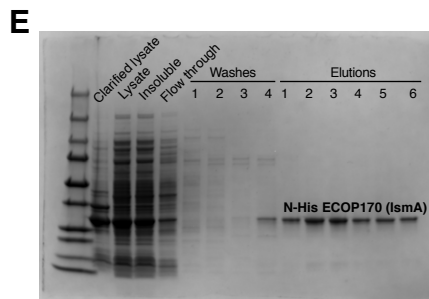
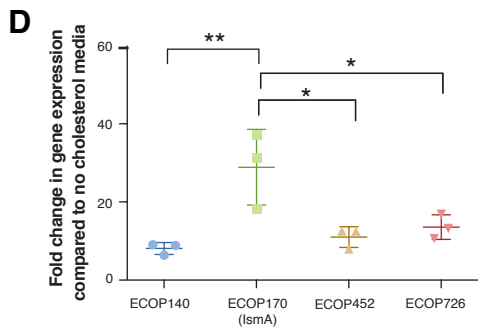
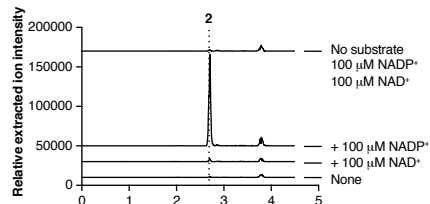
### A. *E. coprostanoligenes* culture



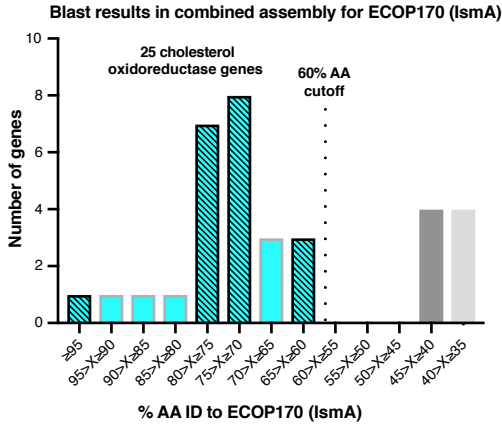
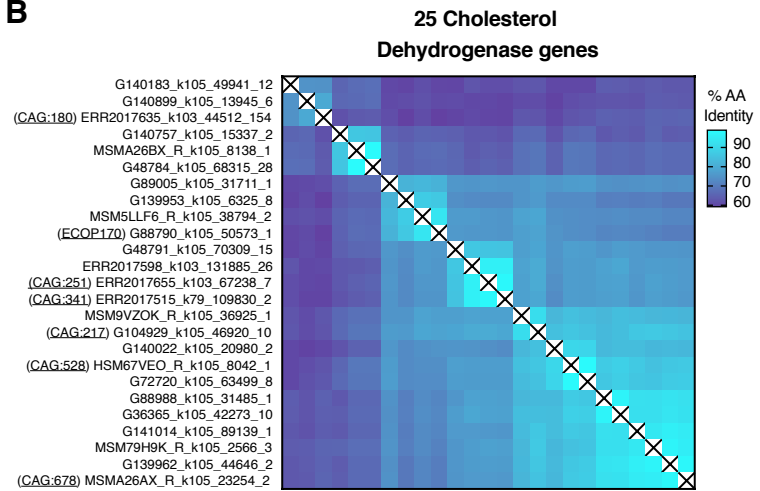
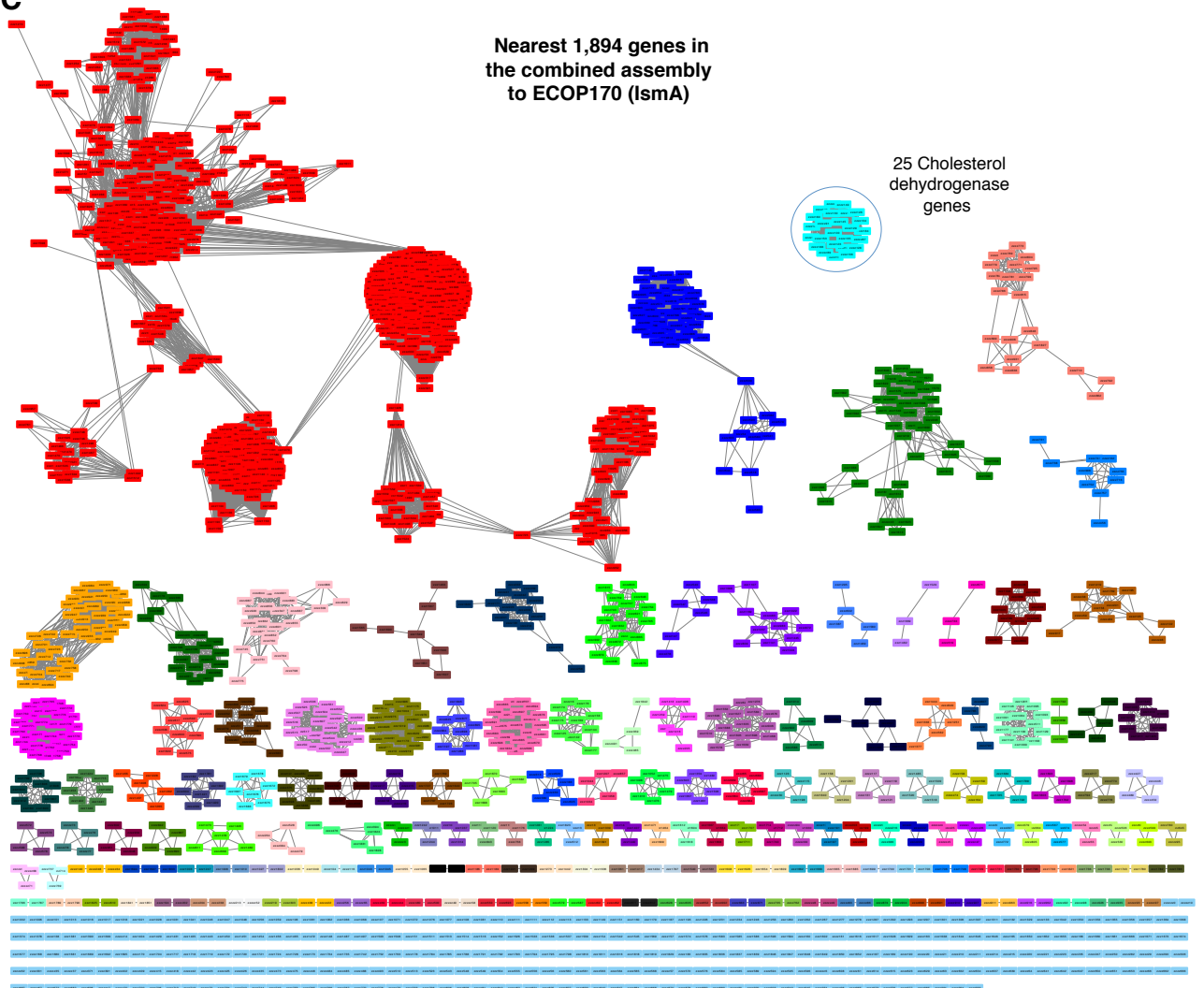
### B. *E. coprostanoligenes* lysate experiments (Oxygen-dependence)



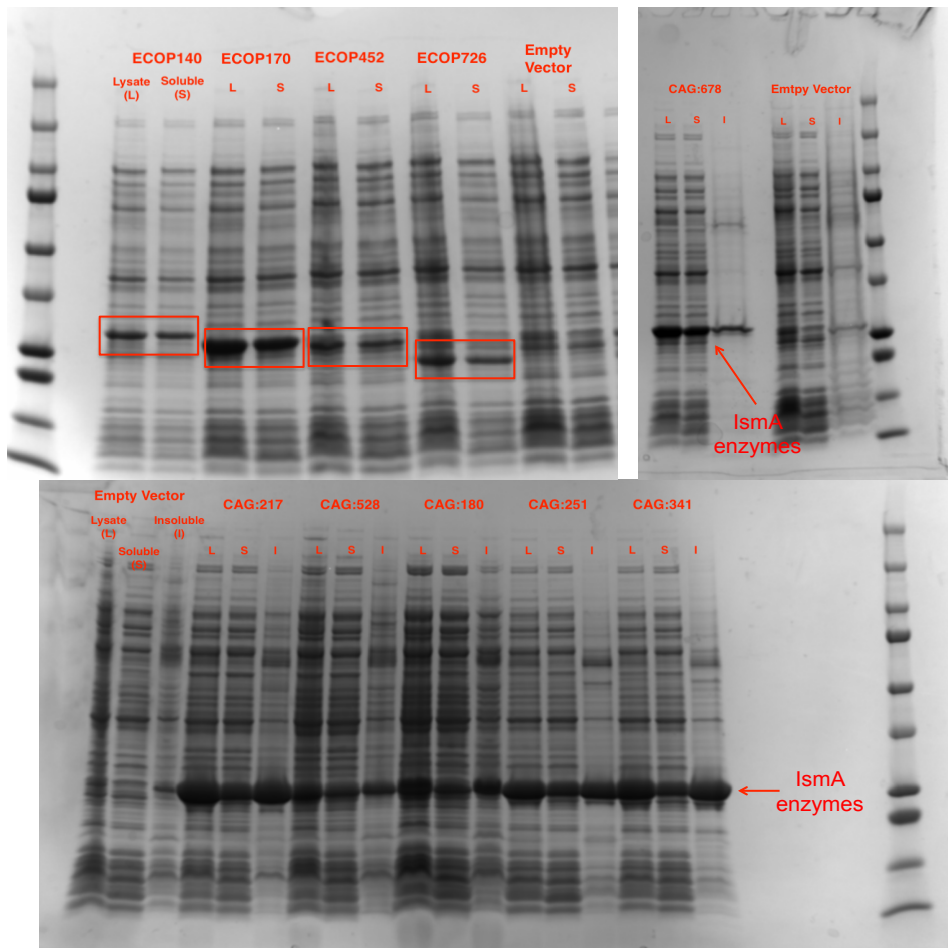
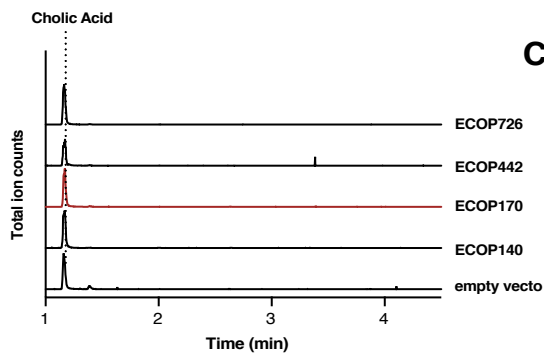
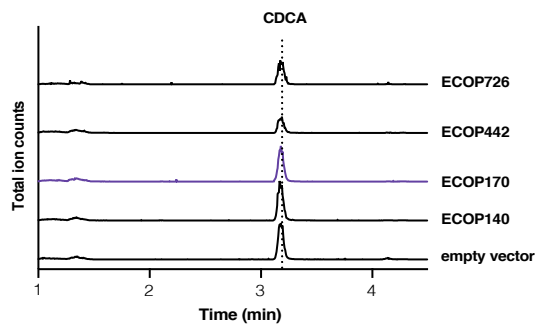
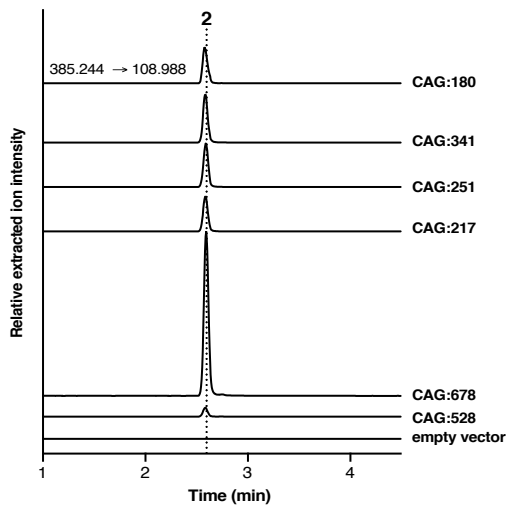
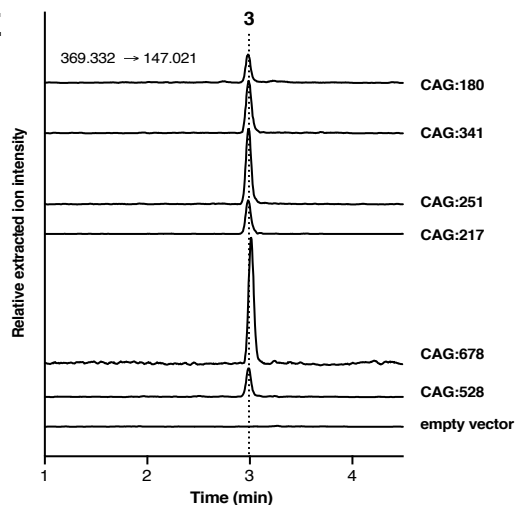
### C. *E. coprostanoligenes* lysate experiment (Anaerobic)



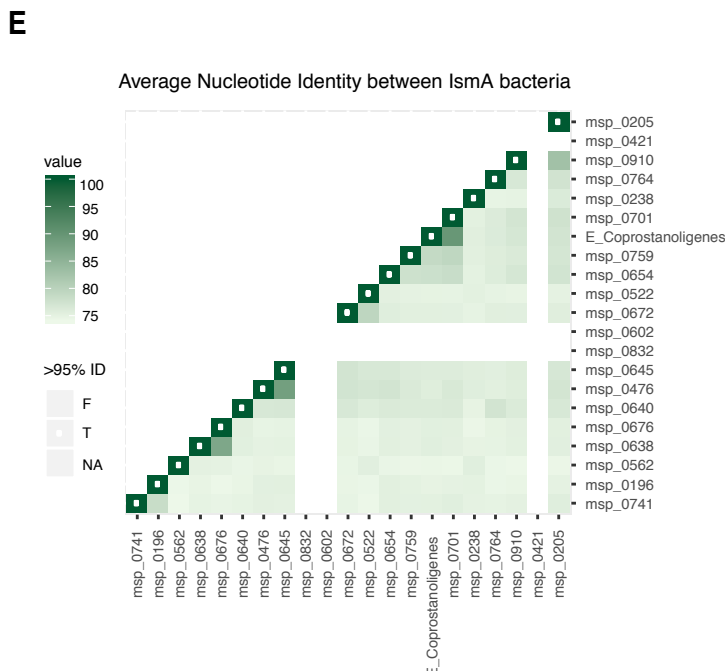
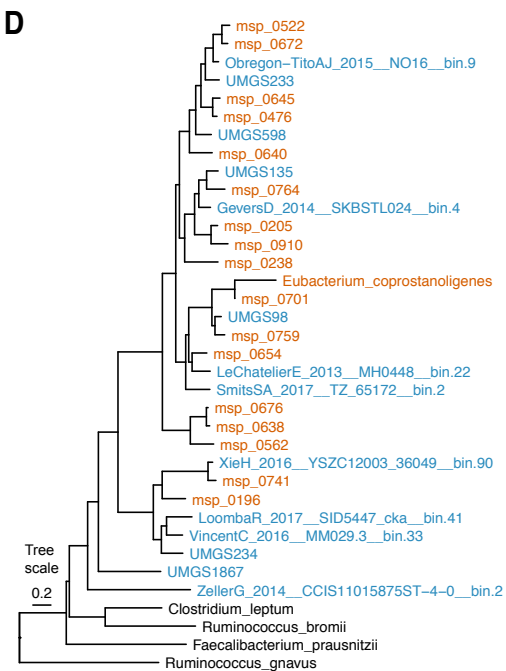
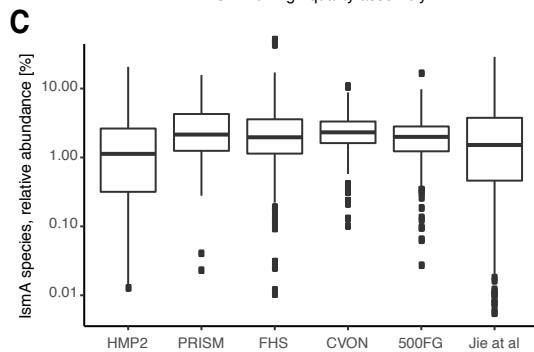
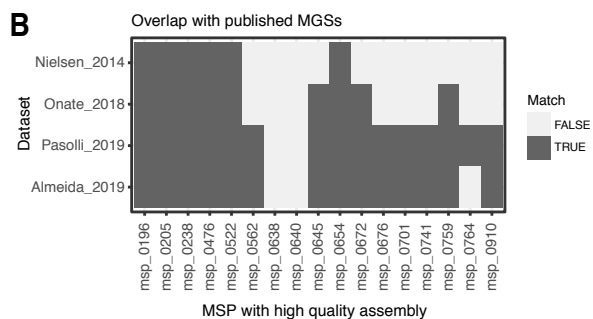
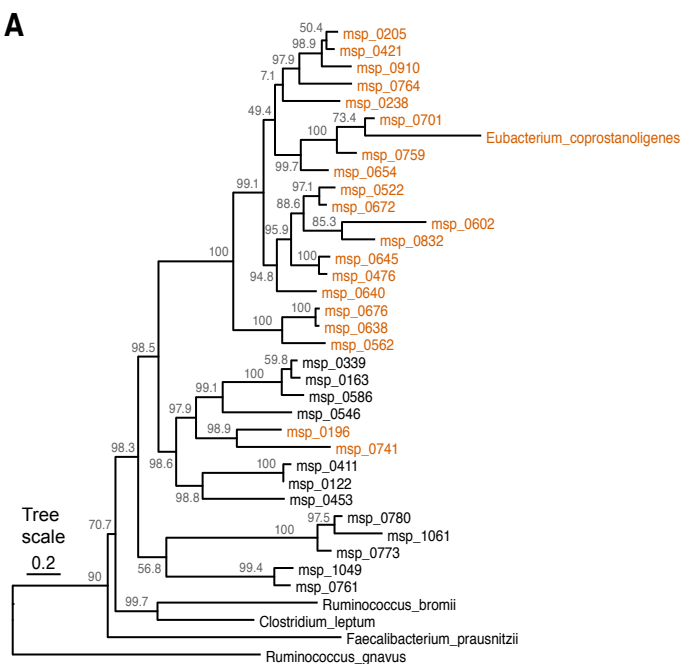
**Figure S3. Identification of human-associated cholesterol dehydrogenases with homology to IsmA in the combined assembly of gut metagenomes from six human cohorts, related to Figure 3. (A)** 1,854 proteins with the highest percent AA identity to ECOP170 were identified. A histogram of the genes with an e-value of less than  $1E-50$  (33 genes) was made. The percent AA identity bins clearly show a gap in sequences between greater than 60% and less than 45% AA identity with ECOP170. The cutoff for putative cholesterol dehydrogenases was therefore set at 60% AA identity. The percent AA identity bins that contain a characterized cholesterol dehydrogenase protein are identified by the black border and diagonal pattern. **(B)** Percent AA identity matrix between all 25 cholesterol dehydrogenase genes found within the combined microbiome assembly. **(C)** A protein sequence similarity network (SSN) was constructed using the 1,854 proteins from the combined assembly with greater than 20% AA identity to ECOP170. Nodes represent proteins with 100% sequence identity. The SSN is displayed with a percent AA identity threshold of 60%. The 25 cholesterol dehydrogenase proteins are circled and shown in light blue.

**A****B****C**

**Figure S4. IsmAs from human-associated gut microbes metabolize cholesterol and coprostanol but not primary bile acids, related to Figure 3. (A)** SDS-PAGE gels showing expression of all HSDs in *E. coli* BL21. Activity assay with *E. coli* lysates (PBS, pH = 7.4) and either **(B)** 100  $\mu$ M of cholic acid or **(C)** 100  $\mu$ M of chenodeoxycholic acid (CDCA) with 100  $\mu$ M each of NAD<sup>+</sup> and NADP<sup>+</sup>. TICs are shown for the duration of the method. No reaction was observed with any lysates tested. Activity assay with *E. coli* lysates (PBS, pH = 7.4) expressing one of the IsmA enzymes from human-associated microbes and either **(D)** 100  $\mu$ M cholesterol or **(E)** 100  $\mu$ M of coprostanol with 100  $\mu$ M each of NAD<sup>+</sup> and NADP<sup>+</sup>. EIC for the products of both reactions are shown.

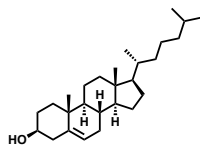
**A****B****C****D****E**

**Figure S5. IsmA-encoding species identified across 6 human gut microbiome cohorts are related to known *Clostridium* species and are associated with coprostanol formation in *ex vivo* stool cultures, related to Figure 4.** (A) Phylogenetic tree as in Fig. 4A with added support values for each split in the tree as calculated by FastTree (Price et al., 2010). (B) High quality genomes of IsmA- encoding MSPs were compared with previously published efforts of cataloguing uncultured species (metagenomic species, MGS) in the human microbiome by global alignment at gene level (USEARCH). MSP was assumed “matched” to an MGS if the majority of its genes mapped with min. 95% DNA identity. For this comparison two gene-centric studies (Nielsen et al., 2014); (Plaza Oñate et al., 2018) and two genome-binning studies (Pasolli et al., 2019); (Almeida et al., 2019) were used. (C) Relative abundance of the IsmA-encoding MSPs quantified across each dataset used in this study. Boxplots show median and lower/upper quartiles, whiskers show inner fences and dots show outliers. (D) Phylogenetic neighbourhood of *Eubacterium coprostanoligenes* including high quality genomes of IsmA-encoding MSPs (orange) and additional 14 IsmA-encoding species from Pasolli et al. and Almeida et al. (blue). Tree was generated using PhyloPhlAn (Segata et al., 2013). (E) The average nucleotide identity (ANI) was computed between the MSPs draft genomes and *E. coprostanoligenes* genome. The three MSPs without a high quality draft genome are left blank. ANI scores between two MSPs that are greater than 95% (likely indicating the same species), are marked with a white rectangle.

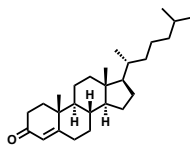
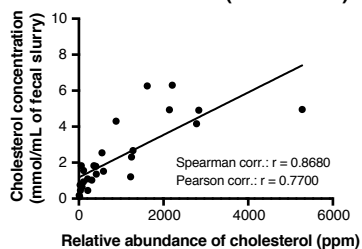




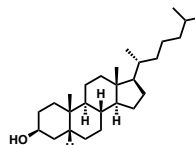
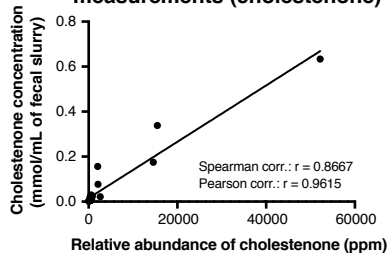
**Figure S6. Quantitative targeted metabolomics of cholesterol, cholestenone and coprostanol in a subset of stool samples from the PRISM cohort, related to Figure 5. (A)** Concentrations of cholesterol, cholestenone and coprostanol were determined by comparison to authentic standards in a standard curve (n=26 samples). The values we obtained for each of these metabolites in a given sample were plotted against their respective relative abundances as determined by untargeted metabolomics methods. Cholesterol (rt 17.573, 369.332 → 147.021), cholestenone (rt 17.652, 385.244 → 108.988), coprostanol (rt 18.899, 371.304 → 95.011). Both Pearson and Spearman coefficients (r) are shown for each metabolite. **(B)** The cutoff for calling coprostanol positive samples was determined by using the mean signal plus 3 standard deviations from the 13 coprostanol negative samples as determined by untargeted metabolomics (mean negative samples = 0.0275 mmol of coprostanol/mL of fecal slurry; std. dev of negative samples = 0.0320 mmol of coprostanol/mL of fecal slurry; cutoff for calling samples coprostanol positive = mean of negative sample + 3SD = 0.1236 mmol of coprostanol/mL of fecal slurry). **(C)** Concentrations of cholesterol, cholestenone and coprostanol in each fecal slurry are shown.

**A**

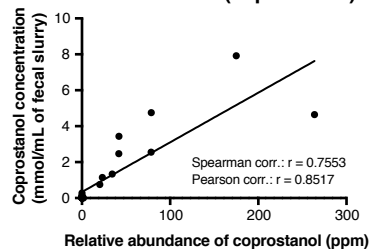
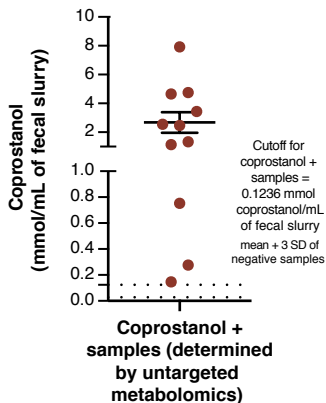
### Validation of metabolomic measurements (cholesterol)



### Validation of metabolomic measurements (cholestenone)



### Validation of metabolomic measurements (coprostanol)

**B****C**